

Motivation

- The OLYMPEX field study over western Washington offers a chance to validate the WRF bulk microphysics during three heavy precipitation events associated with atmospheric rivers.
- The WRF schemes (see setup below) underpredicted precipitation for all three events (Fig. 1), with low-land sites underpredicted early and windward later (Fig. 3), so the question is why? And why the P3 scheme performs slightly better?

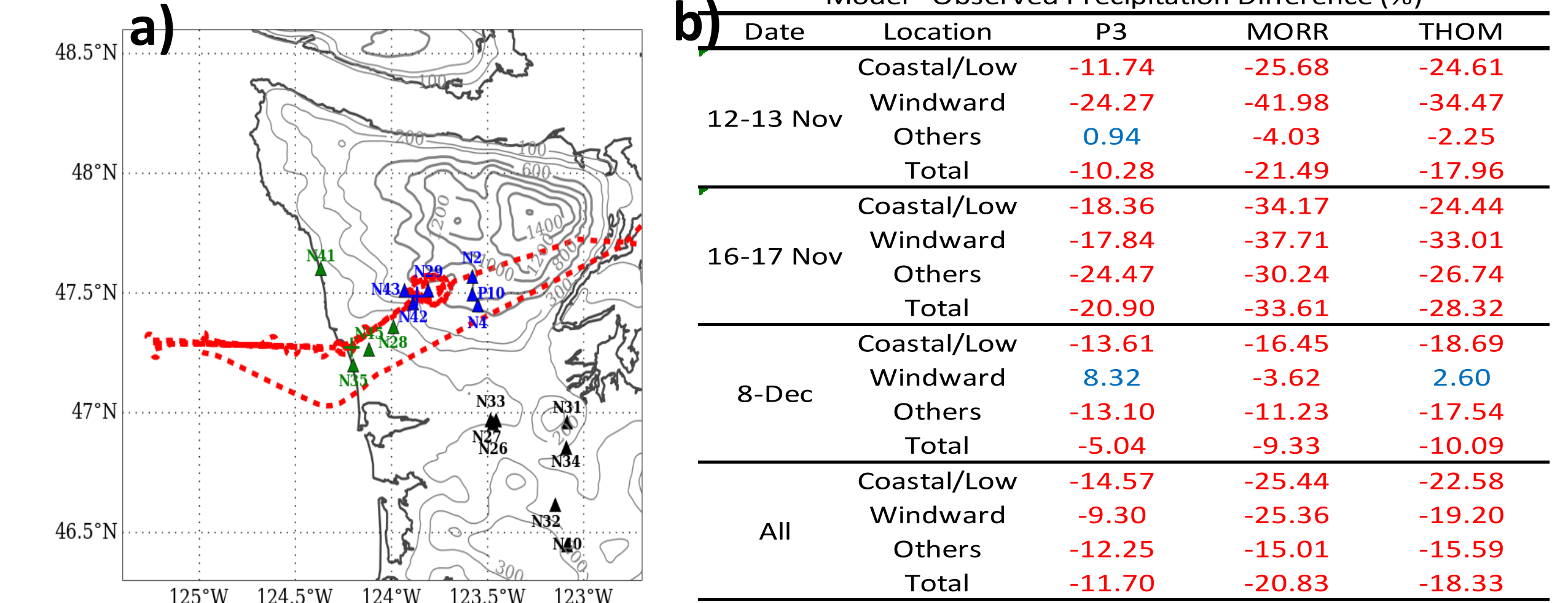
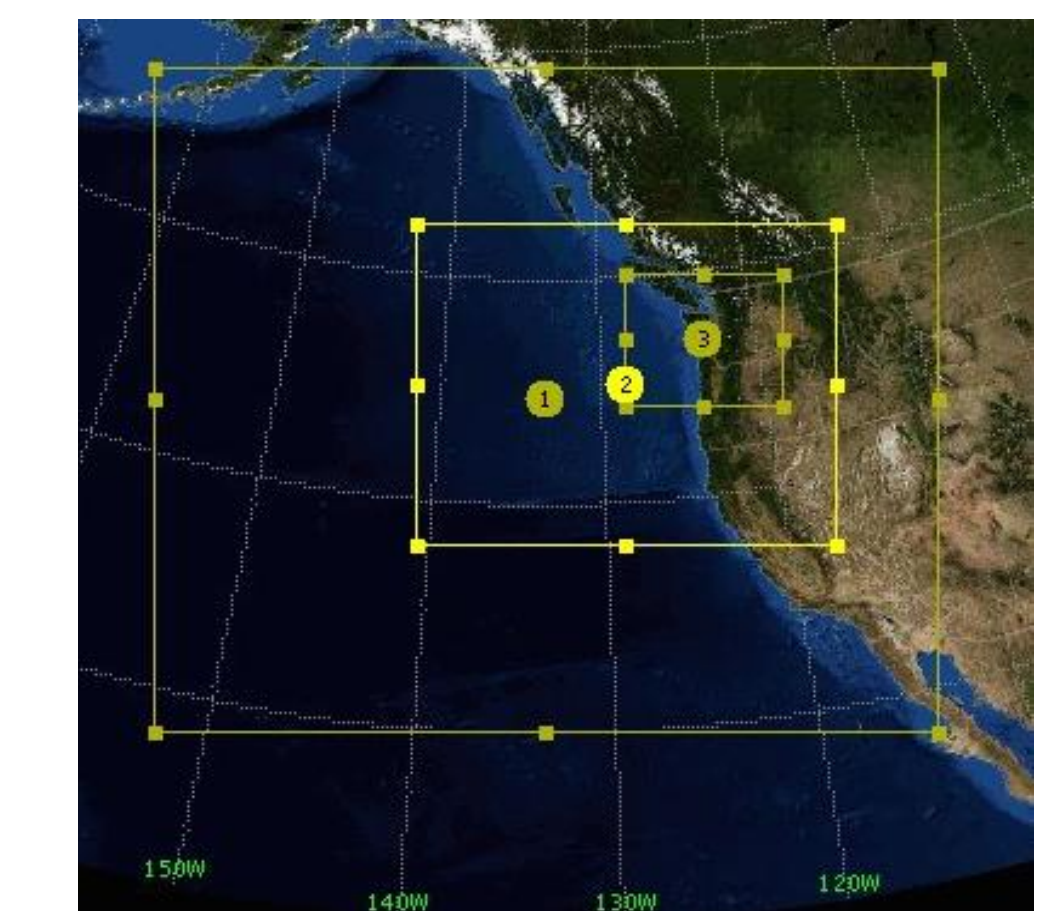


Figure 1. (a) OLYMPEX field domain showing the lowland (green), windward (blue), and other (black) precipitation gauges as well as the flight track from the Citation aircraft for 12-13 November 2015. (b) The percent of observed precipitation for the WRF is shown for each of the three heavy precipitation events with atmospheric rivers and for all 3 events (All), with the results separated by the lowland, windward, and other. Red indicates WRF underprediction.

Model Setup and Configuration



- 3 OLYMPEX cases simulated (12-13 Nov, 17 Nov, 8-9 Dec 2015).
- WRF V3.7.1 at 9, 3, and 1-km grid (50 levels).
- IC/BCs: (6-h 0.25° GFS analyses, RAP, and NARR)
- MYJ PBL, Grell-Freitas (9 km), RRTMG
- 36-h runs starting (11/12/12z, 11/16/12z, and 12/08/00z). First 6 to 9-h spin-up.

Microphysical schemes

- Thompson (THOM)** – (2008) ~2D ice, ice size distribution from Field et al. (2005), variable riming efficiency.
- Morrison (MORR)** – (2009) ~ predicts number concentration (N_x) to get snow/ice size distribution (λ) and intercept (N_{ox}). Spherical snow.
- Predicted Particle Properties (P3)** – Morrison and Milbrandt (2015) Single ice-phase category derives predicted particle properties (e.g., rime mass fraction, bulk density, and mean particle size).
- Hebrew University (HUJI)** – spectral bin microphysics, 33 mass bins for water drops, 3 ice crystals (plate, columnar, branch), aggregates, graupel, and hail/frozen drops

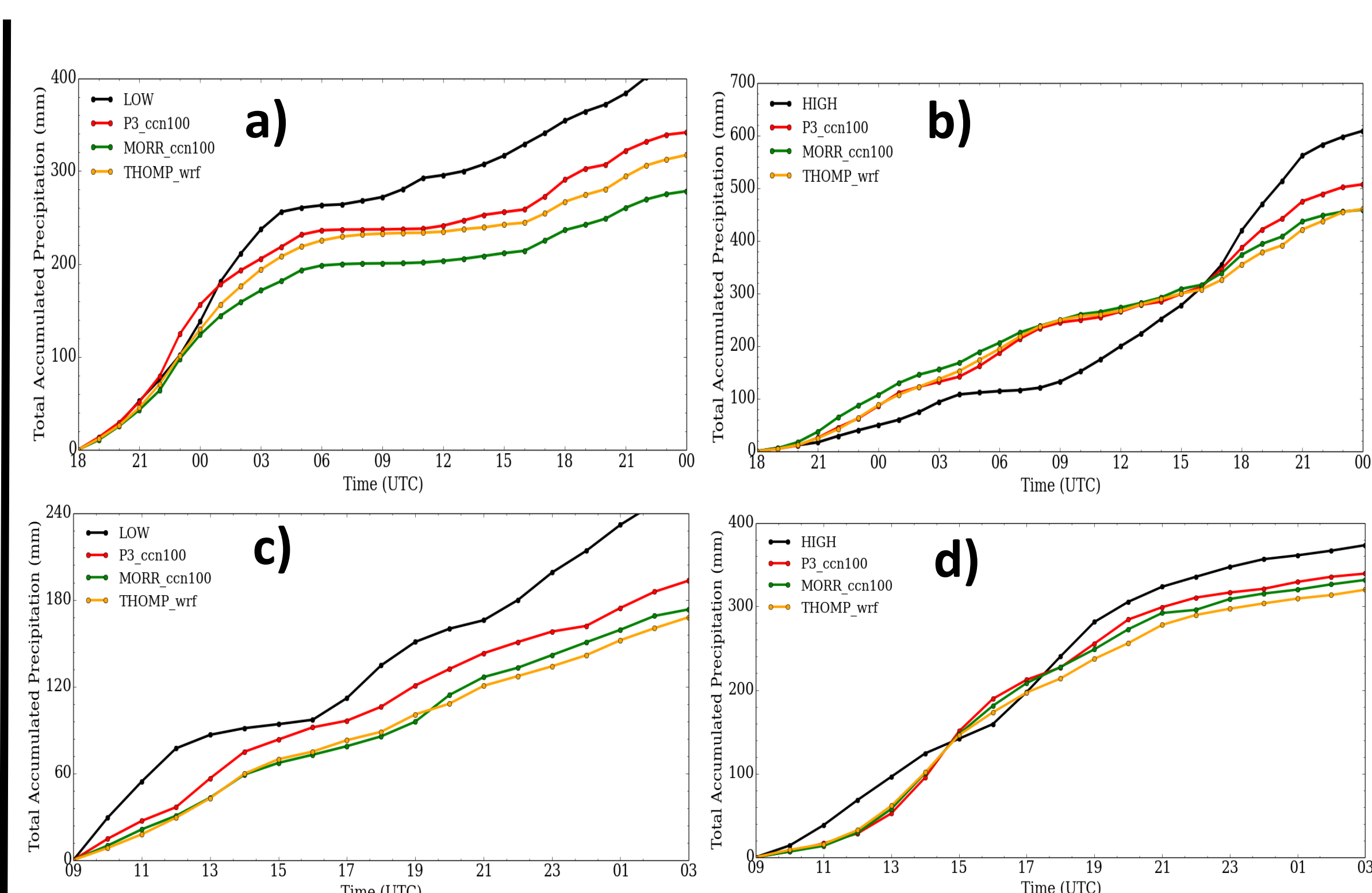
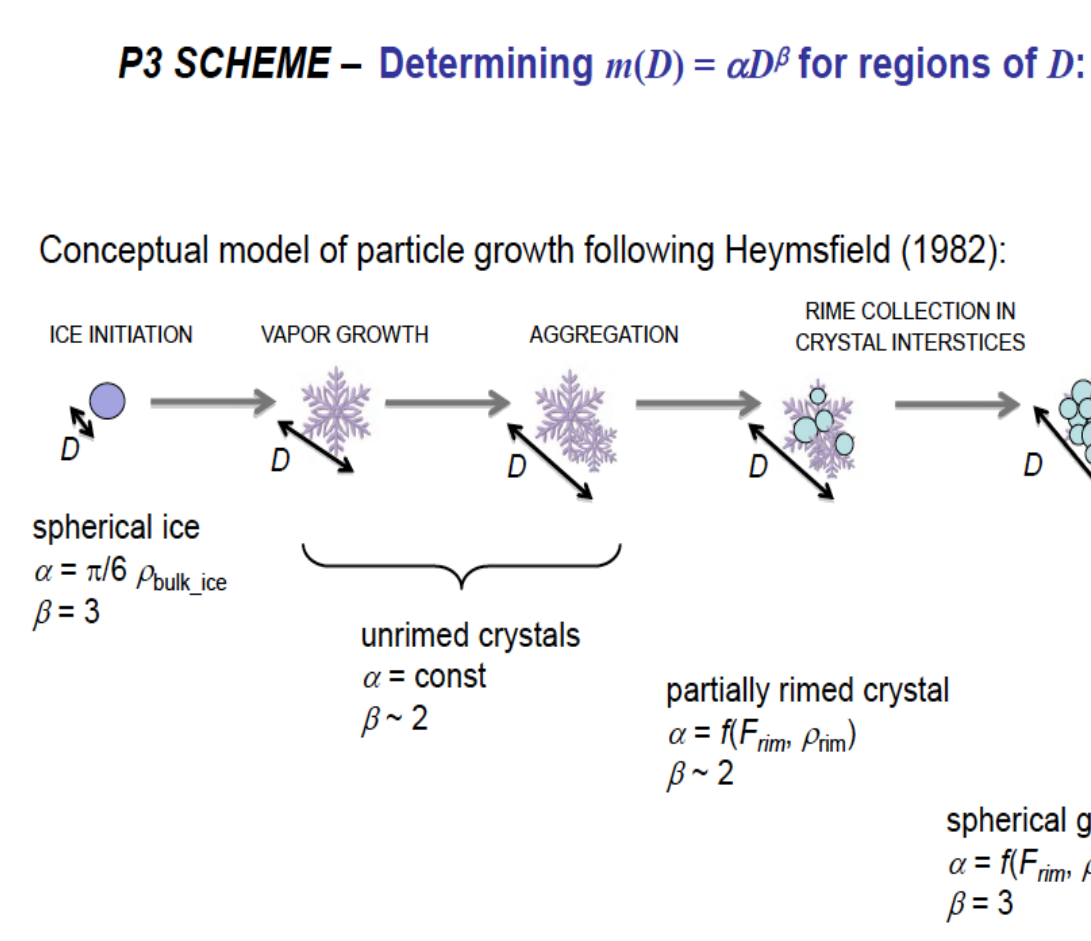


Figure 3. Observed and 1-km WRF BMP precipitation (in mm) summed for the (a) lowland and (b) windward sites for the 16-17 Nov 2015 case. (c-d) Same as (a-b) except for the 8-9 Dec 2015 case. The WRF tends to underpredict for the low-land sites early in the event, while there is a period mid-way through the events in which the windward sites are more underpredicted.

Blocked Flow, Low-level Turbulence

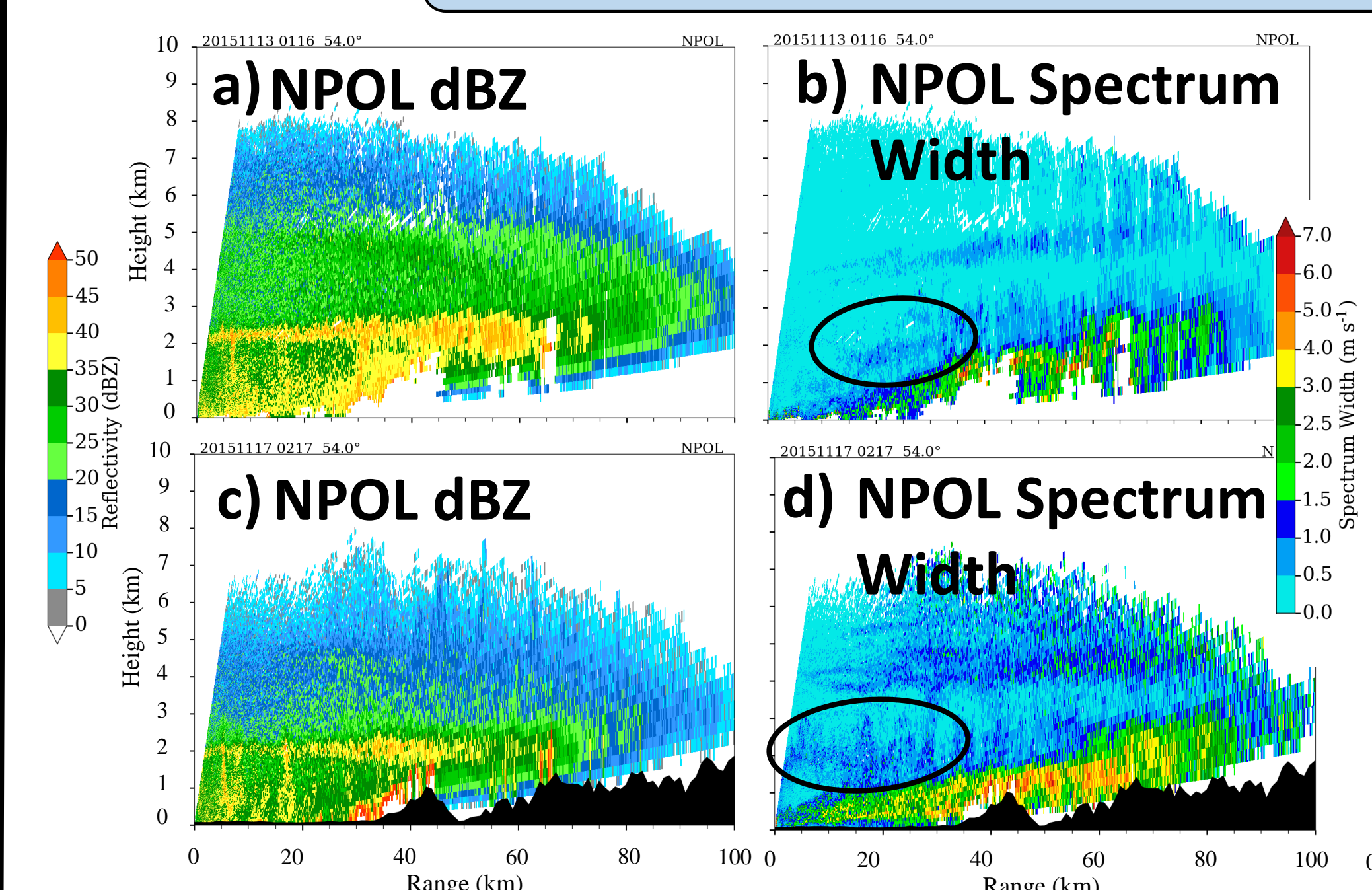


Figure 7. (a) Observed radar reflectivity and (b) spectrum width along NPOL RHI scan at ~01 UTC 13 Nov. (c-d) Same as (a-b) except at ~02 UTC 17 Nov.

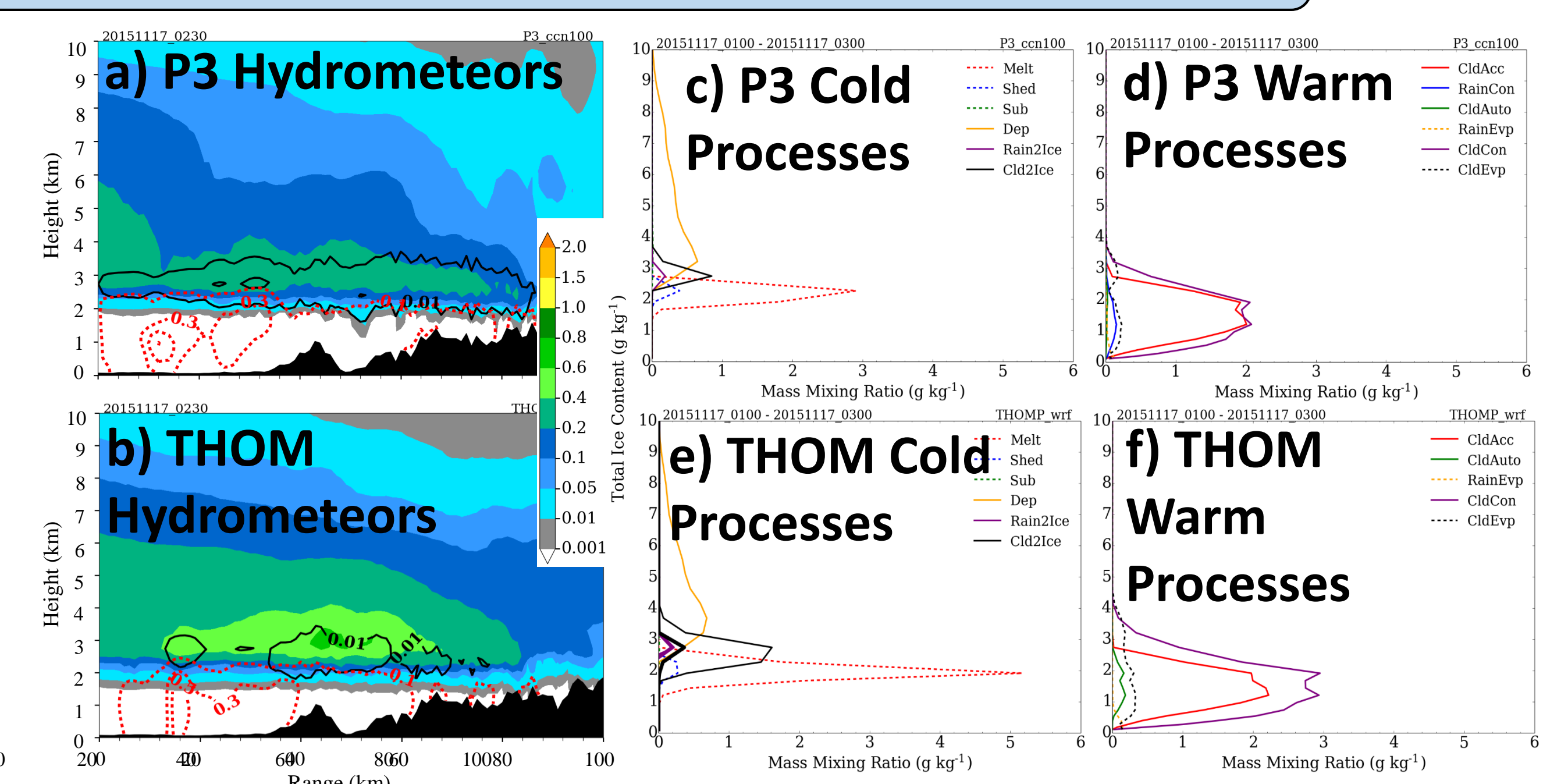


Figure 8. (a) Same as Fig. 5a, except for 0230 UTC 17 Nov. Same as (b) except for THOM. (c-f) P3 and THOM cold and warm-phase processes

- Possible enhancement of ice-phase accretion due to turbulence, especially on 17 Nov. Warm rain likely more dominant on 13 Nov as turbulent layer is primarily below melting level. All BMPs likely underestimating cold rain due to missing turbulence.

Unblocked Flow, Less Stability over Windward Slopes

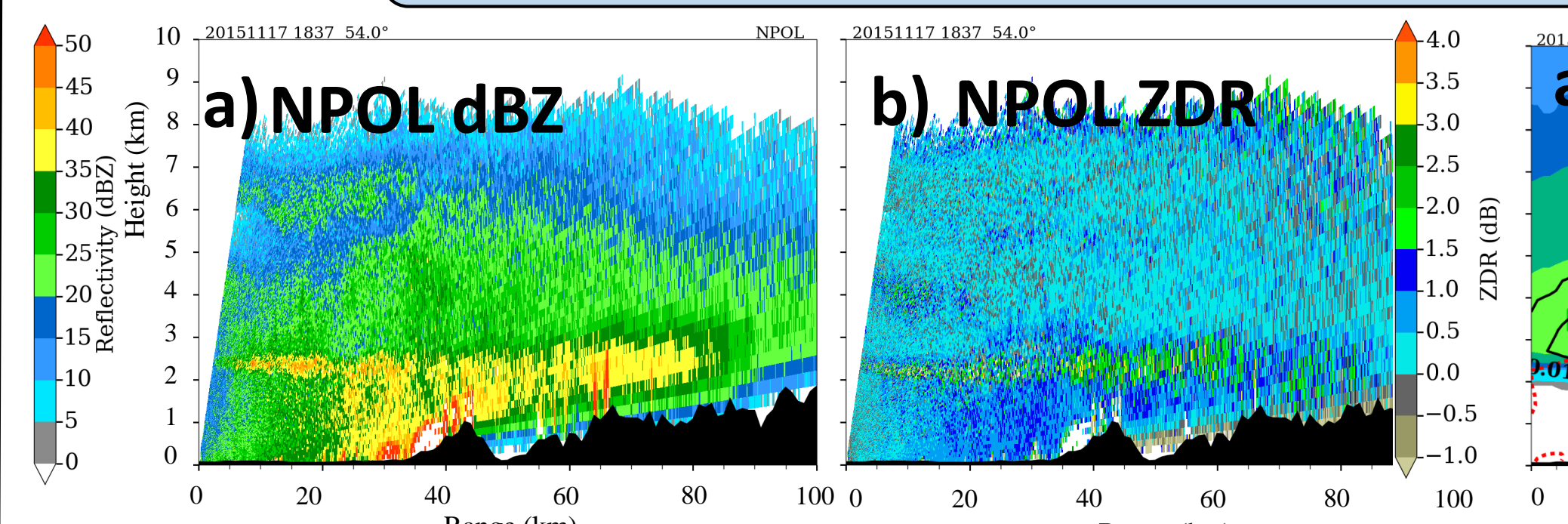


Figure 10. Same as Fig. 4 except valid at ~1840 UTC 17 Nov

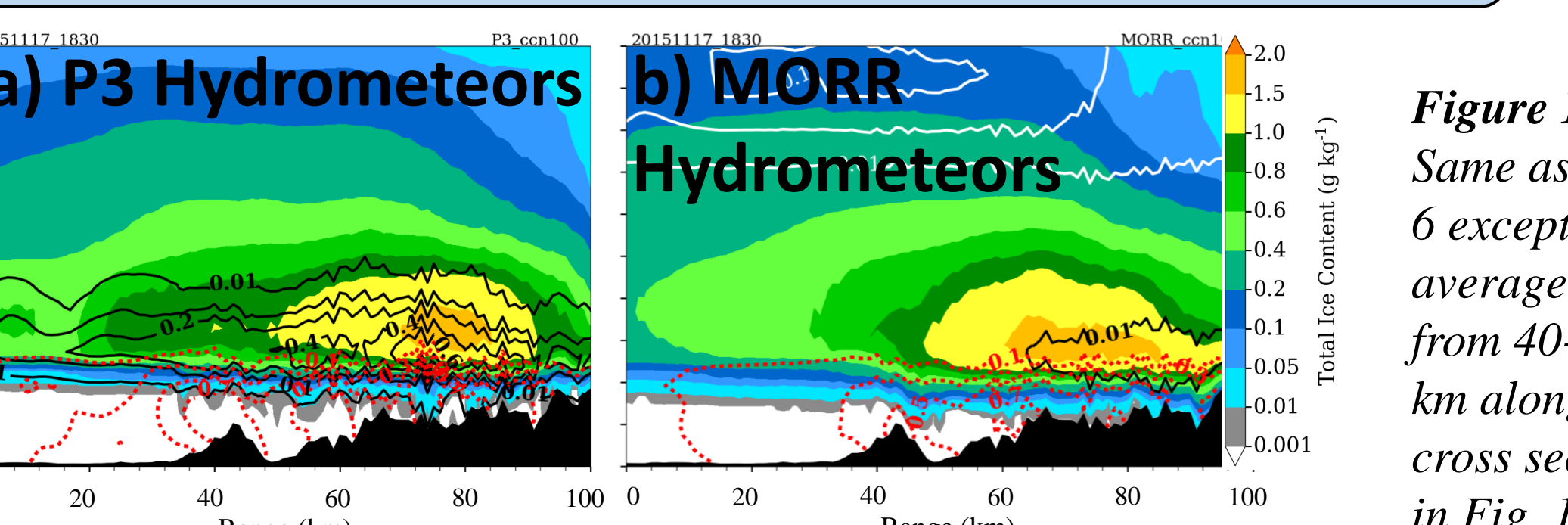


Figure 11. Same as Fig. 5 except valid at 1830 UTC 17 Nov

- P3 simulates more realistic precip over windward slopes due to riming, but underprediction still apparent.

Blocked Flow, Rime Layer

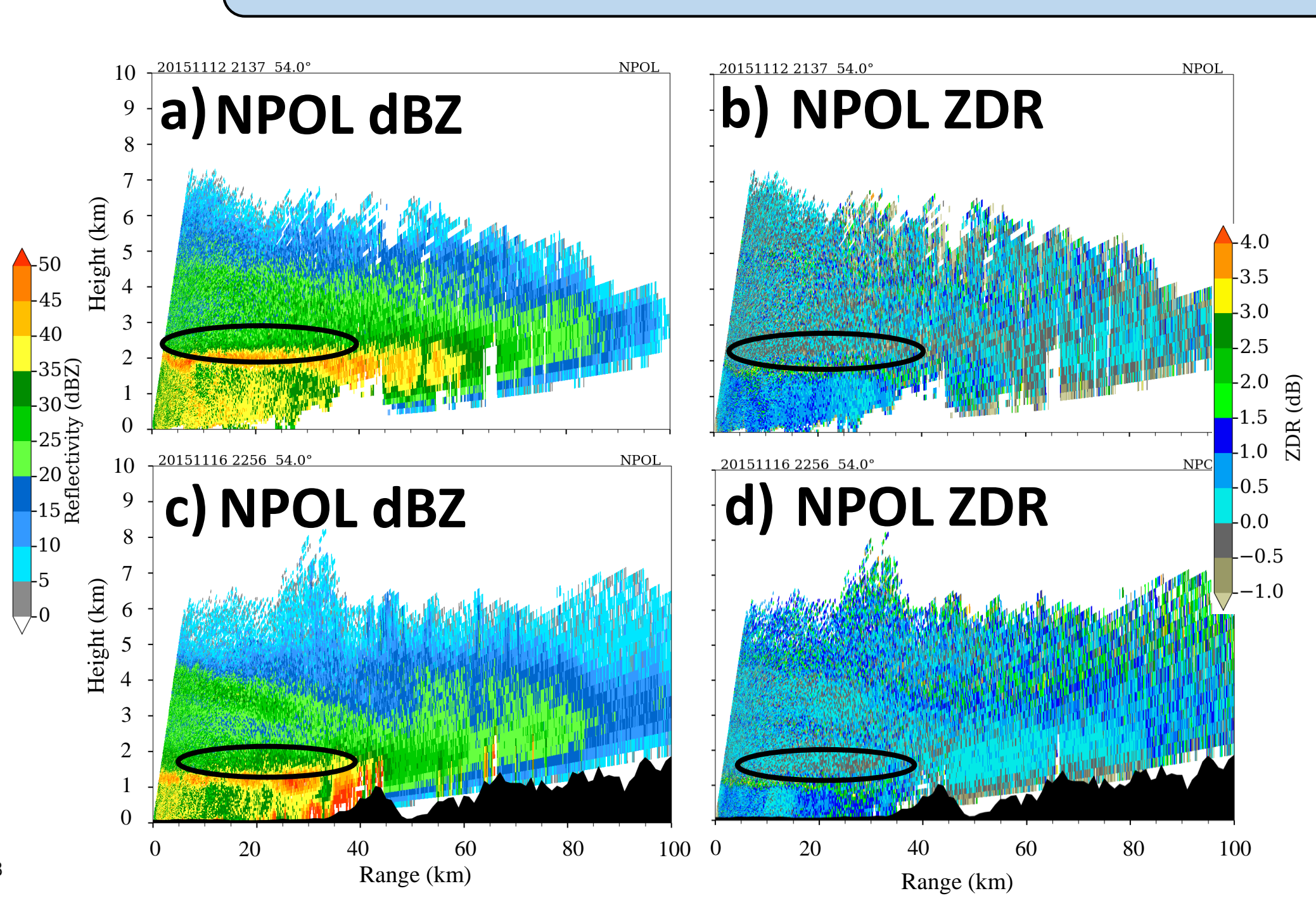


Figure 4. (a) Observed radar reflectivity and (b) differential reflectivity (ZDR) along NPOL RHI scan at ~22 UTC 12 Nov. (c-d) Same as (a-b) except at ~23 UTC 16 Nov.

- NPOL shows near 0 ZDR above strong, saggy bright band, which suggests a layer of rimed particles. P3 predicts most active riming, which leads to faster falling particles, enhanced melting, and cold rain, while MORR and THOM (not shown) predicts larger snow amounts aloft.

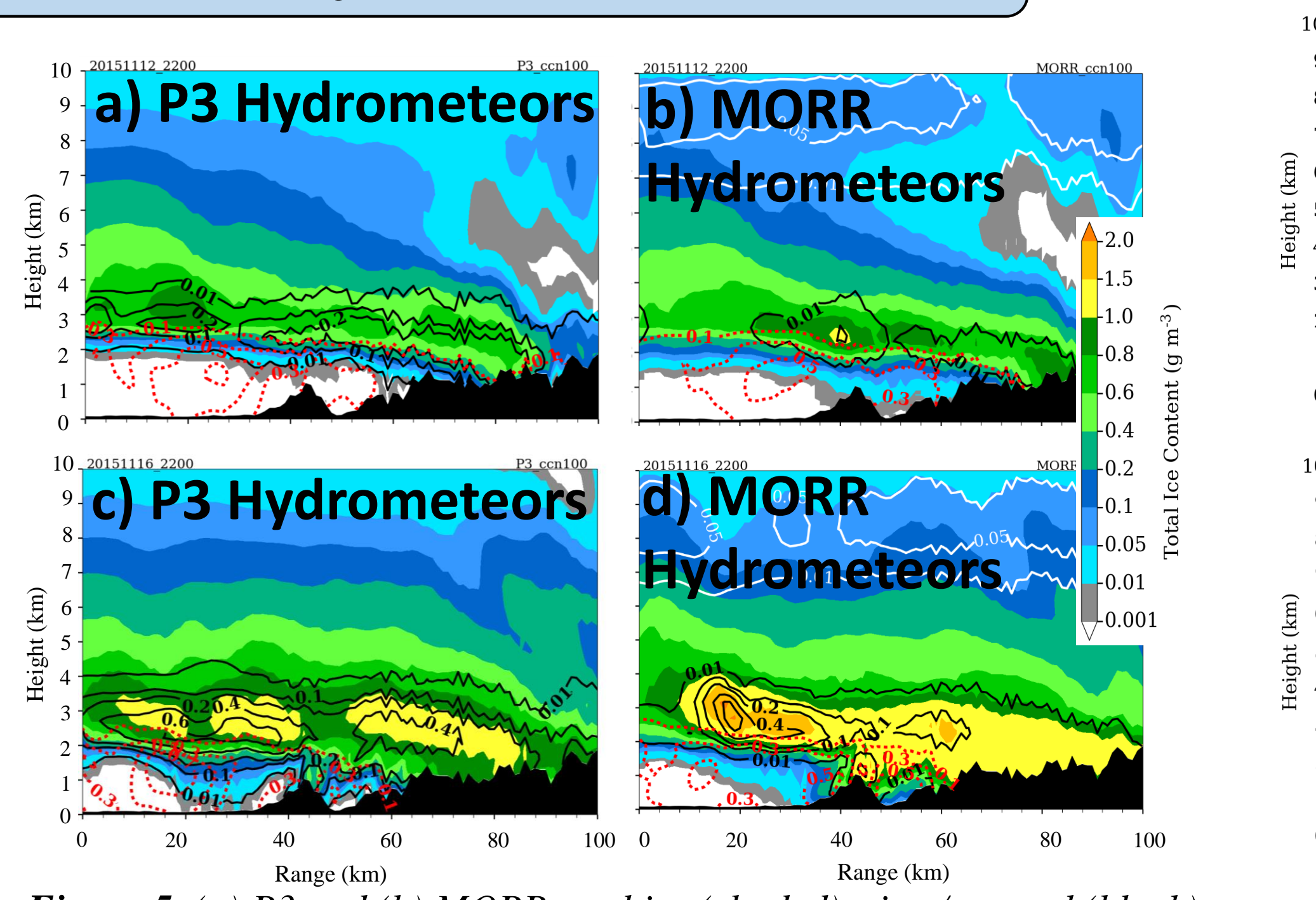


Figure 5. (a) P3 and (b) MORR total ice (shaded), rime/graupel (black), rain (red), and ice mass (white) at 22 UTC 12 Nov. Note P3 does not have separate ice mass category. (c-d) Same as (a-b) except for MORR.

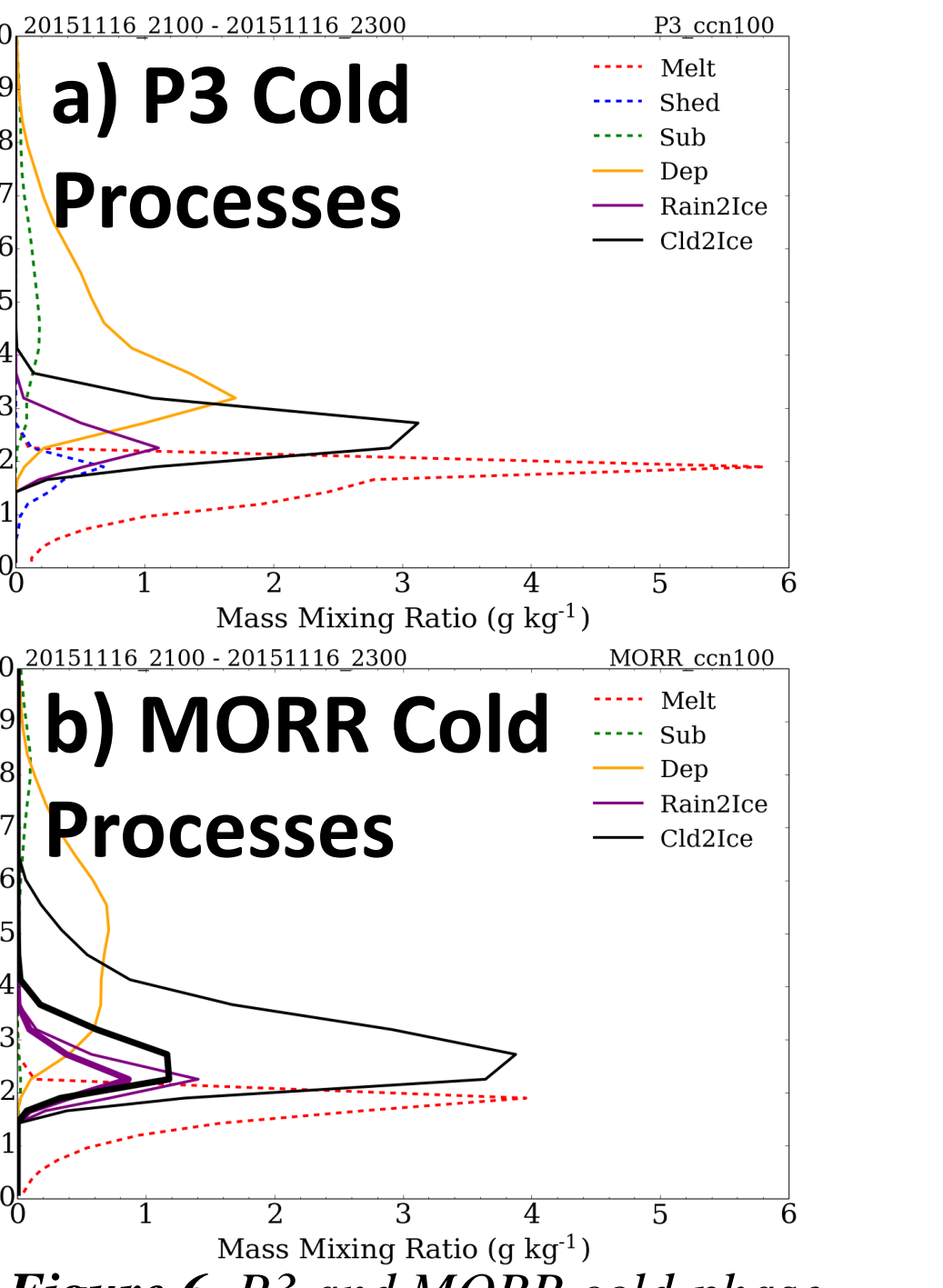


Figure 6. P3 and MORR cold-phase processes averaged from 0 to 30 km along the model cross sections in Fig. 5.

Low Terrain Hydrometeor Properties

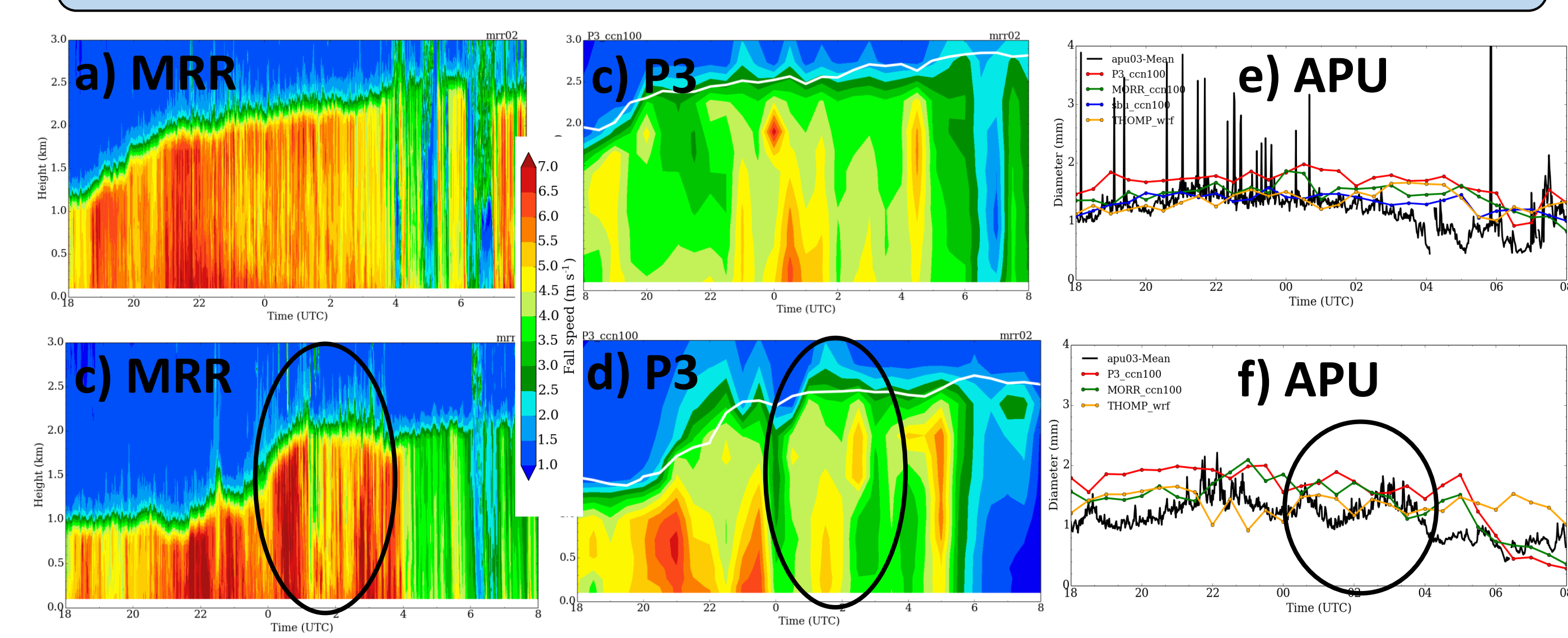


Figure 9. (a) Micro Rain Radar (MRR) fall velocities at Fishery valid at 18 UTC 12 Nov. (b) P3 fall velocities during same time period as (a). (c-d) Same as (a-b) except valid at 18 UTC 16 Nov. (e) APU mass-weighted rain diameter at Fishery on 12 Nov. (f) Same as (e) except on 16 Nov.

- Underprediction in all BMP fall velocities due to limited riming aloft.

Windward Hydrometeor Properties

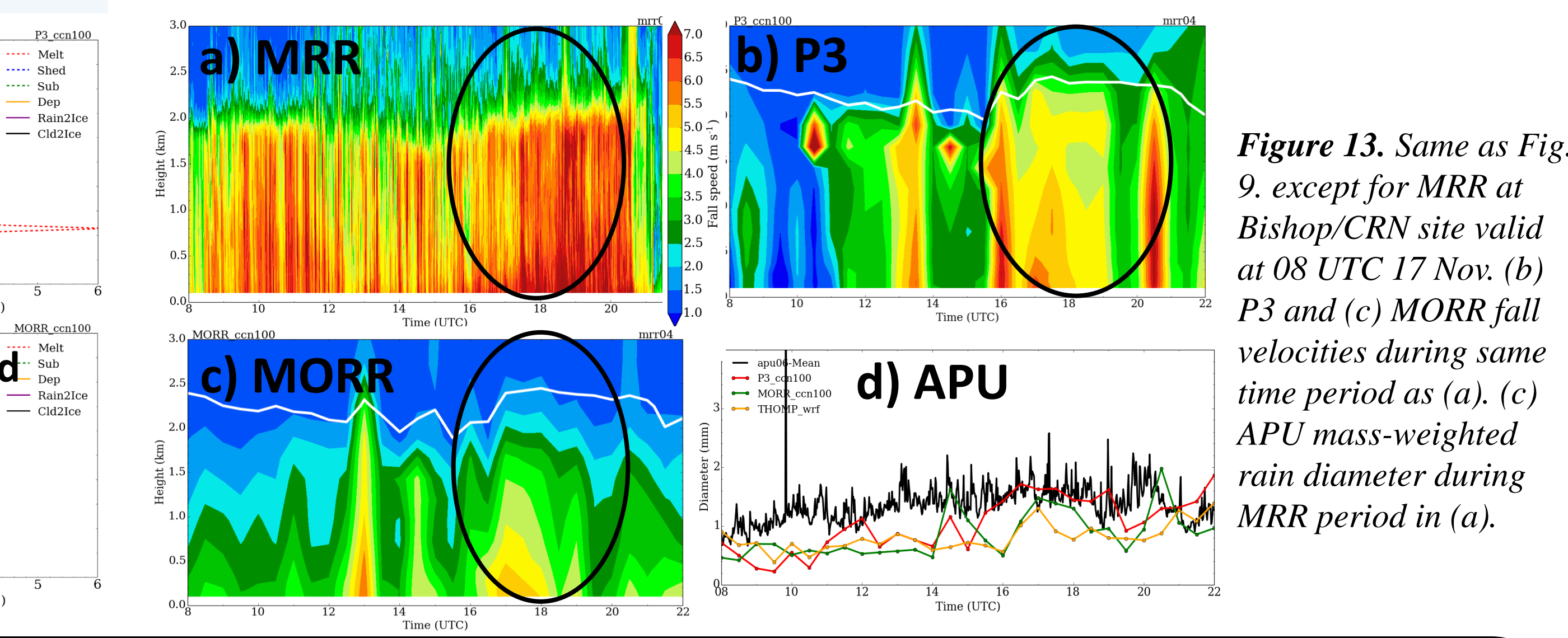


Figure 13. Same as Fig. 9, except for MRR at Bishop/CRN site valid at 08 UTC 17 Nov. (b) P3 and (c) MORR fall velocities during same time period as (a). (d) APU mass-weighted rain diameter during MRR period in (a).

Summary and Future Work

P3 generally predicts more active riming processes than other BMPs, which can lead to more realistic precipitation rates as indicated by intensive validation data during atmospheric river events during OLYMPEX. The more active riming processes lead to higher fall speeds, larger rain diameters, and precipitation production. However, missing low-level turbulence parameterizations in the BMPs can lead to precipitation underprediction in stable, blocked flow conditions. We plan to conduct LES simulations down to 50-100 m grid spacing to help quantify the impact of turbulence on microphysics and precipitation in the BMP schemes. Simulations of past field campaign events will also be utilized to conduct a broader validation of the BMPs.